ELSEVIER

International Journal of Solids and Structures 41 (2004) 2643–2657

INTERNATIONAL JOURNAL OF SOLIDS and STRUCTURES

www.elsevier.com/locate/ijsolstr

Postbuckling prediction of double-walled carbon nanotubes under hydrostatic pressure

Hui-Shen Shen

School of Civil Engineering and Mechanics, Shanghai Jiao Tong University, 1954 Hua Shan Road, Shanghai 200030, People's Republic of China

Received 12 March 2003; received in revised form 7 November 2003

Abstract

An elastic double-shell model is presented for the buckling and postbuckling of a double-walled carbon nanotube subjected to external hydrostatic pressure. The analysis is based on a continuum mechanics model in which each tube of a double-walled carbon nanotube is described as an individual elastic shell and the interlayer friction is negligible between the inner and outer tubes. The governing equations are based on higher order shear deformation shell theory with a von Kármán–Donnell-type of kinematic nonlinearity. The van der Waals interaction between the inner and outer nanotubes and the nonlinear prebuckling deformations of the shell are both taken into account. A boundary layer theory of shell buckling is extended to the case of double-walled carbon nanotubes under hydrostatic pressure. A singular perturbation technique is employed to determine the buckling loads and postbuckling equilibrium paths. Numerical results reveal that the single-walled carbon nanotube has a stable postbuckling path, whereas the double-walled carbon nanotube has an unstable postbuckling behavior due to the presence of van der Waals interaction forces.

Keywords: Buckling; Postbuckling; Nanotube; Continuum shell model; Higher order shear deformable shell theory; Boundary layer theory of shell buckling; Singular perturbation technique

1. Introduction

Carbon nanotubes have received considerable attention in many areas of science and industry since they were first reported in 1991 (Iijima, 1991). Carbon nanotubes are cylindrical macromolecules composed of carbon atoms in a periodic hexagonal arrangement. Carbon nanotubes possess extraordinary physical properties such as high stiffness-to-weight and strength-to-weight ratios and enormous electrical and thermal conductivities. Many believe that carbon nanotubes may provide the ultimate reinforcing materials for the development of a new class of nanocomposites (see, Thostenson et al., 2001; Qian et al., 2002). To realize the potential benefits, fundamental understanding of carbon nanotubes is required. Many studies on the material properties of single-walled and/or multi-walled carbon nanotubes under hydrostatic pressure

E-mail address: hsshen@mail.sjtu.edu.cn (H.-S. Shen).

0020-7683/$ - see front matter © 2003 Elsevier Ltd. All rights reserved.
doi:10.1016/j.ijsolstr.2003.11.028

have been performed, see, for example Reich et al. (2000, 2002), Tang et al. (2000, 2002) and Liu et al. (2001). Buckling phenomenon was described by singularities in the strain energy profile (Yakobson et al., 1996). Two theoretical approaches to understanding and predicting the buckling behavior of carbon nanotubes are atomistic molecular-dynamics simulations and continuum mechanics (see Yakobson et al., 1996; Wong et al., 1997; Ru, 2000a; Das and Wille, 2002; Harik, 2002). Yakobson et al. (1996) presented a molecular-dynamics simulation of single-walled carbon nanotubes under axial buckling, bending and torsion, but they did not simulate nanotubes under hydrostatic pressure. Molecular-dynamics simulations have provided abundant results for the understanding of buckling behaviors of carbon nanotubes. However, molecular-dynamics simulations are currently limited to very small length and time scales and cannot deal with the large-sized atomic system, due to the limitations of current computing power. Moreover, at the nanoscale, experiments are extremely difficult and expensive to conduct. So far, no buckling experiments have been reported for nanotubes under external hydrostatic pressure. As a result, the continuum mechanics models are expected for the theoretical analysis of buckling behavior of carbon nanotubes.

The importance of the van der Waals interaction and its role in the energetic and elastic deformation of ''molecular'' systems have been extensively discussed (Ruoff et al., 1993; Hertel et al., 1998). Ru (2000b, 2001) proposed a continuum shell model to study compressive buckling of a double-walled carbon nanotube in the presence of the intertube van der Waals forces, but his solutions are approximate due to the assumption of equally axial stress resultants of the outer and inner tubes. Recently, Wang et al. (2003a,b) extend the Ru's continuum shell model to the case of multi-walled carbon nanotubes under radial pressure and combined loading. In these studies, the classical shell theory, i.e. the theory based on the Kirchhoff–Love hypothesis, is used and therefore the transverse shear deformation is usually not accounted for. It is well known this theory is adequate for cylindrical shells when the radius-to-thickness ratio is greater than 20. It has been shown (Yakobson et al., 1996; Das and Wille, 2002; Liu and Chen, 2003), most carbon nanotubes have low values of radius-to-thickness ratio. As a result, the continuum mechanics model for multi-walled carbon nanotubes requires the use of shear deformation shell theory and involves an interlayer van der Waals interaction. To study the maximum bearing loading under large strain, nonlinear postbuckling behavior of carbon nanotubes has to be investigated.

The main objective of the present study is to predict the postbuckling behavior of double-walled carbon nanotubes subjected to hydrostatic pressure. In the present study all thermal, quantum and electromagnetic effects are neglected. Following Ru (2000b, 2001) an elastic double-shell model is proposed and each tube is described as an individual elastic shell and the interlayer friction is negligible between the inner and outer tubes. The governing equations are based on higher order shear deformation shell theory with a von Kármán–Donnell-type of kinematic nonlinearity. The boundary layer theory for shell buckling suggested by Shen and Chen (1988, 1990) is extended to the case of double-walled carbon nanotubes. A singular perturbation technique is employed to determine the buckling loads and postbuckling equilibrium paths. The nonlinear prebuckling deformations of the shell and the van der Waals interaction forces are both taken into account. The numerical illustrations show the full nonlinear postbuckling response of a double-walled carbon nanotube under hydrostatic pressure, although a comparison is still not available due to the lack of relevant experimental results or molecular-dynamics simulations.

2. Theoretical development

Consider a double-walled carbon nanotube modeled as a shell system which is subjected to external pressure q. The outer and inner tubes are assumed to have the same thickness t, length L and effective material constants E and v, and have mean radii R_I and R_{II}, respectively, as shown in Fig. 1. Each shell is referred to a coordinate system (X, Y, Z) in which X and Y are in the axial and circumferential directions of the shell and Z is in the direction of the inward normal to the middle surface. The corresponding dis-

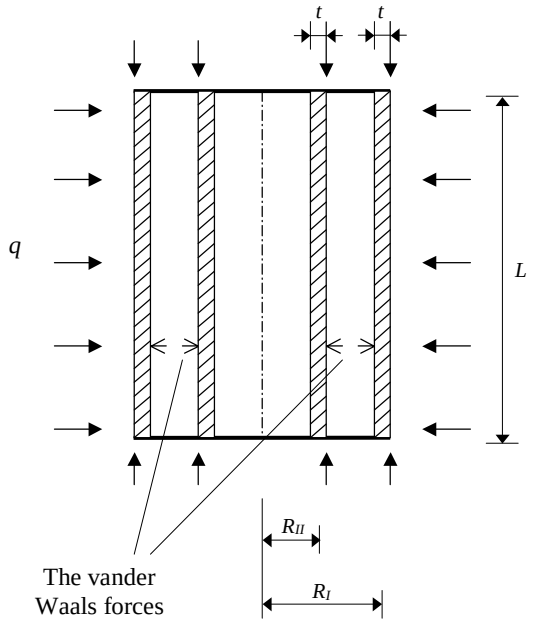

Fig. 1. An elastic shell model for a double-walled carbon nanotube under hydrostatic pressure.

placements are designated by $\overline{U}$, $\overline{V}$ and $\overline{W}$. $\bar{\Psi}_x$ and $\bar{\Psi}_y$ are the rotations of normals to the middle surface with respect to the Y- and X-axes, respectively. The origin of the coordinate system is located at the end of each shell on the middle plane. Let $\overline{W}(X,Y)$ be the transverse deflection of each tube, and $\overline{F}(X,Y)$ be the stress function for the stress resultants defined by $\overline{N}_x = \overline{F}_{,yy}$, $\overline{N}_y = \overline{F}_{,xx}$ and $\overline{N}_{xy} = -\overline{F}_{,xy}$, where a comma denotes partial differentiation with respect to the corresponding coordinates.

The van der Waals interaction potential, as a function of interlayer spacing between adjacent tubes, can be estimated by the Lennard-Jones model (see Girifalco and Lad, 1956; Girifalco, 1991). Using a method described in Girifalco and Lad (1956) and Girifalco (1991), the van der Waals force exerted on any atom on a tube can be estimated by adding up all forces between the atom and all atoms on the other tube. To this end, the interaction forces between the inner and outer shells can be assumed to be a function of the normal distance between the inner and outer tubes at that point, i.e. $p = p_0 + C[\overline{W}_{\mathrm{II}}(X,Y) - \overline{W}_{\mathrm{I}}(X,Y)]$, in which and what follows the subscript I and II refer to the outer and inner tubes, respectively. p_0 is a constant representing the initial uniform van der Waals pressure between two prior to buckling, and C is a constant which can be estimated as the second derivative of the van der Waals energy-interlayer spacing. In particular, the equilibrium distance between a carbon atom and a flat monolayer is around 0.34 nm (Girifalco and Lad, 1956), so that the initial pressure p_0 between the inner and outer tubes is zero or negligible if the initial interlayer spacing is 0.34 nm.

It has been shown (Cumings and Zettl, 2000; Kolmogorov and Crespi, 2000) the friction energy barrier between adjacent tubes is so low that the tubes could almost freely slid and rotate toward each other. We assume that no sliding occurs between the outer and inner tubes. We also assume that the tube is empty, and no initial internal pressure exists. Based on higher order shear deformation shell theory (Reddy and Liu, 1985), the Kármán–Donnell-type nonlinear differential equations for the outer tube, including van der Waals interaction forces, have readily been derived and can be expressed in terms of a stress function $\overline{F}_{\mathrm{I}}$, two rotations $\bar{\Psi}_{x\mathrm{I}}$ and $\bar{\Psi}_{y\mathrm{I}}$, and two transverse displacements $\overline{W}_{\mathrm{I}}$ and $\overline{W}_{\mathrm{II}}$. They are

$$\widetilde{L}_{11}(\overline{W}_{\mathrm{I}}) - \widetilde{L}_{12}(\bar{\Psi}_{x\mathrm{I}}) - \widetilde{L}_{13}(\bar{\Psi}_{y\mathrm{I}}) - \frac{1}{R_{\mathrm{I}}}\overline{F}_{\mathrm{I},xx} = \widetilde{L}(\overline{W}_{\mathrm{I}}, \overline{F}_{\mathrm{I}}) + p_0 + C(\overline{W}_{\mathrm{II}} - \overline{W}_{\mathrm{I}}) + q \tag{1}$$

$$\widetilde{L}_{21}(\overline{F}_{\mathrm{I}}) + \frac{1}{R_{\mathrm{I}}}\overline{W}_{\mathrm{I},xx} = -\frac{1}{2}\widetilde{L}(\overline{W}_{\mathrm{I}}, \overline{W}_{\mathrm{I}}) \tag{2}$$

$$\widetilde{L}_{31}(\overline{W}_{\mathrm{I}}) + \widetilde{L}_{32}(\bar{\Psi}_{x\mathrm{I}}) - \widetilde{L}_{33}(\bar{\Psi}_{y\mathrm{I}}) = 0 \tag{3}$$

$$\widetilde{L}_{41}(\overline{W}_{\mathrm{I}}) - \widetilde{L}_{42}(\bar{\Psi}_{x\mathrm{I}}) + \widetilde{L}_{43}(\bar{\Psi}_{y\mathrm{I}}) = 0 \tag{4}$$

and for the inner tube they are

$$\widetilde{L}_{11}(\overline{W}_{\mathrm{II}}) - \widetilde{L}_{12}(\bar{\Psi}_{x\mathrm{II}}) - \widetilde{L}_{13}(\bar{\Psi}_{y\mathrm{II}}) - \frac{1}{R_{\mathrm{II}}}\overline{F}_{\mathrm{II},xx} = \widetilde{L}(\overline{W}_{\mathrm{II}}, \overline{F}_{\mathrm{II}}) - \frac{R_{\mathrm{I}}}{R_{\mathrm{II}}}[p_0 + C(\overline{W}_{\mathrm{II}} - \overline{W}_{\mathrm{I}})] \tag{5}$$

$$\widetilde{L}_{21}(\overline{F}_{\mathrm{II}}) + \frac{1}{R_{\mathrm{II}}}\overline{W}_{\mathrm{II},xx} = -\frac{1}{2}\widetilde{L}(\overline{W}_{\mathrm{II}}, \overline{W}_{\mathrm{II}}) \tag{6}$$

$$\widetilde{L}_{31}(\overline{W}_{\mathrm{II}}) + \widetilde{L}_{32}(\bar{\Psi}_{x\mathrm{II}}) - \widetilde{L}_{33}(\bar{\Psi}_{y\mathrm{II}}) = 0 \tag{7}$$

$$\widetilde{L}_{41}(\overline{W}_{\mathrm{II}}) - \widetilde{L}_{42}(\bar{\Psi}_{x\mathrm{II}}) + \widetilde{L}_{43}(\bar{\Psi}_{y\mathrm{II}}) = 0 \tag{8}$$

where the linear operators $\widetilde{L}_{ij}(\ )$ and the nonlinear operator $\widetilde{L}(\ )$ are defined as in Shen (2001). Because the nanotubes are assumed to be isotropic, the shell stiffnesses used in these operators will have $A^*_{ij} = A^{-1}_{ij} = (Et)^{-1}$ and $D^*_{ij} = D_{ij} = D = Et^3/[12(1-\nu^2)]$. Note that Eqs. (1)–(8) are coupled and should be solved simultaneously.

The two end edges of both outer and inner tubes are assumed to be simply supported or clamped, so that the boundary conditions are $X = 0, L$:

$$\overline{W} = \bar{\Psi}_y = 0 \tag{9a}$$

$$\overline{M}_x = \overline{P}_x = 0 \quad \text{(simply supported)} \tag{9b}$$

$$\bar{\Psi}_x = 0 \quad \text{(clamped)} \tag{9c}$$

$$\int_0^{2\pi R_{\mathrm{I}}} \overline{N}_{x\mathrm{I}}\,\mathrm{d}Y + \int_0^{2\pi R_{\mathrm{II}}} \overline{N}_{x\mathrm{II}}\,\mathrm{d}Y + \pi R_{\mathrm{I}}^2 q = 0 \tag{9d}$$

where $\overline{M}_x$ is the bending moment and $\overline{P}_x$ is higher order moment, as defined in Reddy and Liu (1985). Also we have the closed (or periodicity) condition for each tube

$$\int_0^{2\pi R_{\mathrm{I}}} \frac{\partial \overline{V}}{\partial Y}\,\mathrm{d}Y = 0 \tag{10a}$$

or

$$\int_0^{2\pi R_{\mathrm{I}}} \left[\frac{1}{Et}\left(\frac{\partial^2 \overline{F}}{\partial X^2} - \nu\frac{\partial^2 \overline{F}}{\partial Y^2}\right) + \frac{\overline{W}}{R_{\mathrm{I}}} - \frac{1}{2}\left(\frac{\partial \overline{W}}{\partial Y}\right)^2\right]\mathrm{d}Y = 0 \tag{10b}$$

Because of Eq. (10a), the in-plane boundary condition $\overline{V} = 0$ (at $X = 0, L$) is not needed in Eq. (9a).

It is assumed that the end-shortening displacements of the outer and inner tubes are identical. The average end-shortening relationship of each shell is defined as

$$\frac{\Delta_x}{L} = -\frac{1}{2\pi R_J L}\int_0^{2\pi R_J}\int_0^{L}\frac{\partial \overline{U}}{\partial X}\,\mathrm{d}X\,\mathrm{d}Y$$
$$= -\frac{1}{2\pi R_J L}\int_0^{2\pi R_J}\int_0^{L}\left[\frac{1}{Et}\left(\frac{\partial^2 \overline{F}}{\partial Y^2} - \nu\frac{\partial^2 \overline{F}}{\partial X^2}\right) - \frac{1}{2}\left(\frac{\partial \overline{W}}{\partial X}\right)^2\right]\mathrm{d}X\,\mathrm{d}Y \quad (J = \mathrm{I}, \mathrm{II}) \tag{11}$$

where Δ_x is shell end-shortening displacement in the X-direction.

3. Analytical method and asymptotic solutions

Having developed the theory, we are in a position to solve Eqs. (1)–(8) with boundary conditions (9). Before proceeding, it is convenient first to define the following dimensionless quantities [with γ_{ijk} in Eqs. (21) and (A.3) below are defined as in Shen (2001)]

$$x = \pi\frac{X}{L}, \quad y = \frac{Y}{R_\mathrm{I}}, \quad \beta = \frac{L}{\pi R_\mathrm{I}}, \quad \varepsilon = \frac{\pi^2 R_\mathrm{I} t}{L^2[12(1-\nu^2)]^{1/2}}, \quad \gamma_0 = \frac{R_\mathrm{II}}{R_\mathrm{I}}, \quad C_0 = \frac{CL^4}{\pi^4 D}, \quad C_1 = \frac{p_0 R_\mathrm{I}}{Et\beta^2}$$
$$W = \varepsilon\frac{\overline{W}}{t}[12(1-\nu^2)]^{1/2}, \quad F = \varepsilon^2\frac{\bar{F}}{D}, \quad (\Psi_x, \Psi_y) = \varepsilon^2\frac{L}{\pi}\frac{(\bar{\Psi}_x, \bar{\Psi}_y)}{t}[12(1-\nu^2)]^{1/2}$$
$$(M_x, P_x) = \varepsilon^2\frac{L^2}{\pi^2}\frac{[12(1-\nu^2)]^{1/2}}{Dt}\left(\overline{M}_x, \frac{4}{3t^2}\overline{P}_x\right), \quad q_\mathrm{cl} = \frac{1}{3}\left(\frac{2}{3}\right)^{1/2}\frac{\pi E}{(1-\nu^2)^{3/4}}\frac{R_\mathrm{I}}{L}\left(\frac{t}{R_\mathrm{I}}\right)^{5/2} \tag{12}$$
$$\lambda_q = \frac{q}{q_{cl}}, \quad \delta_q = \frac{(\Delta_x/L)}{\frac{1}{3}\left(\frac{2}{3}\right)^{1/2}\frac{\pi}{(1-\nu^2)^{3/4}}\frac{R_\mathrm{I}}{L}\left(\frac{t}{R_\mathrm{I}}\right)^{3/2}}$$

The nonlinear equations (1)–(8) may then be written in dimensionless form as

$$\varepsilon^2[L_{11}(W_\mathrm{I}) - C_0(W_\mathrm{II} - W_\mathrm{I})] - \varepsilon L_{12}(\Psi_{x\mathrm{I}}) - \varepsilon L_{13}(\Psi_{y\mathrm{I}}) - F_{\mathrm{I},xx} = \beta^2 L(W_\mathrm{I}, F_\mathrm{I}) + C_1 + \frac{4}{3}(3)^{1/4}\lambda_q\varepsilon^{3/2} \tag{13}$$

$$L_{21}(F_\mathrm{I}) + W_{\mathrm{I},xx} = -\frac{1}{2}\beta^2 L(W_\mathrm{I}, W_\mathrm{I}) \tag{14}$$

$$\varepsilon L_{31}(W_\mathrm{I}) + L_{32}(\Psi_{x\mathrm{I}}) - L_{33}(\Psi_{y\mathrm{I}}) = 0 \tag{15}$$

$$\varepsilon L_{41}(W_\mathrm{I}) - L_{42}(\Psi_{x\mathrm{I}}) + L_{43}(\Psi_{y\mathrm{I}}) = 0 \tag{16}$$

and

$$\varepsilon^2[\gamma_0 L_{11}(W_\mathrm{II}) + C_0(W_\mathrm{II} - W_\mathrm{I})] - \varepsilon\gamma_0 L_{12}(\Psi_{x\mathrm{II}}) - \varepsilon\gamma_0 L_{13}(\Psi_{y\mathrm{II}}) - F_{\mathrm{II},xx} = \gamma_0\beta^2 L(W_\mathrm{II}, F_\mathrm{II}) - C_1 \tag{17}$$

$$\gamma_0 L_{21}(F_\mathrm{II}) + W_{\mathrm{II},xx} = -\frac{1}{2}\gamma_0\beta^2 L(W_\mathrm{II}, W_\mathrm{II}) \tag{18}$$

$$\varepsilon L_{31}(W_\mathrm{II}) + L_{32}(\Psi_{x\mathrm{II}}) - L_{33}(\Psi_{y\mathrm{II}}) = 0 \tag{19}$$

$$\varepsilon L_{41}(W_\mathrm{II}) - L_{42}(\Psi_{x\mathrm{II}}) + L_{43}(\Psi_{y\mathrm{II}}) = 0 \tag{20}$$

where

$$
\begin{aligned}
L_{11}(\ ) &= \gamma_{110}\frac{\partial^4}{\partial x^4} + 2\gamma_{112}\beta^2\frac{\partial^4}{\partial x^2\,\partial y^2} + \gamma_{114}\beta^4\frac{\partial^4}{\partial y^4}\\
L_{12}(\ ) &= \gamma_{120}\frac{\partial^3}{\partial x^3} + \gamma_{122}\beta^2\frac{\partial^3}{\partial x\,\partial y^2}\\
L_{13}(\ ) &= \gamma_{131}\beta\frac{\partial^3}{\partial x^2\,\partial y} + \gamma_{133}\beta^3\frac{\partial^3}{\partial y^3}\\
L_{21}(\ ) &= \frac{\partial^4}{\partial x^4} + 2\beta^2\frac{\partial^4}{\partial x^2\,\partial y^2} + \beta^4\frac{\partial^4}{\partial y^4}\\
L_{31}(\ ) &= \gamma_{31}\frac{\partial}{\partial x} + \gamma_{310}\frac{\partial^3}{\partial x^3} + \gamma_{312}\beta^2\frac{\partial^3}{\partial x\,\partial y^2}\\
L_{32}(\ ) &= \gamma_{31} - \gamma_{320}\frac{\partial^2}{\partial x^2} - \gamma_{322}\beta^2\frac{\partial^2}{\partial y^2}\\
L_{33}(\ ) &= \gamma_{331}\beta\frac{\partial^2}{\partial x\,\partial y}\\
L_{41}(\ ) &= \gamma_{41}\beta\frac{\partial}{\partial y} + \gamma_{411}\beta\frac{\partial^3}{\partial x^2\,\partial y} + \gamma_{413}\beta^3\frac{\partial^3}{\partial y^3}\\
L_{42}(\ ) &= L_{33}(\ )\\
L_{43}(\ ) &= \gamma_{41} - \gamma_{430}\frac{\partial^2}{\partial x^2} - \gamma_{432}\beta^2\frac{\partial^2}{\partial y^2}\\
L(\ ) &= \frac{\partial^2}{\partial x^2}\frac{\partial^2}{\partial y^2} - 2\frac{\partial^2}{\partial x\,\partial y}\frac{\partial^2}{\partial x\,\partial y} + \frac{\partial^2}{\partial y^2}\frac{\partial^2}{\partial x^2}
\end{aligned}
\tag{21}
$$

The boundary conditions of Eq. (9) become

$x = 0, \pi$:

$$W = \Psi_y = 0 \tag{22a}$$

$$M_x = P_x = 0 \quad \text{(simply supported)} \tag{22b}$$

$$\Psi_x = 0 \quad \text{(clamped)} \tag{22c}$$

$$\frac{1}{2\pi}\int_0^{2\pi}\beta^2\frac{\partial^2 F_{\mathrm{I}}}{\partial y^2}\,\mathrm{d}y + \frac{1}{2\pi}\int_0^{2\pi\gamma_0}\beta^2\frac{\partial^2 F_{\mathrm{II}}}{\partial y^2}\,\mathrm{d}y + \frac{2}{3}(3)^{1/4}\lambda_q\varepsilon^{3/2} = 0 \tag{22d}$$

and the closed condition of Eq. (10b) becomes

$$\int_0^{2\pi}\left[\left(\frac{\partial^2 F_{\mathrm{I}}}{\partial x^2} - \nu\beta^2\frac{\partial^2 F_{\mathrm{I}}}{\partial y^2}\right) + W_{\mathrm{I}} - \frac{1}{2}\beta^2\left(\frac{\partial W_{\mathrm{I}}}{\partial y}\right)^2\right]\mathrm{d}y = 0 \tag{23}$$

The unit end-shortening relationship becomes

$$\delta_q = -\frac{(3)^{3/4}}{8\pi^2}\varepsilon^{-3/2}\int_0^{2\pi}\int_0^{\pi}\left[\left(\beta^2\frac{\partial^2 F_{\mathrm{I}}}{\partial y^2} - \nu\frac{\partial^2 F_{\mathrm{I}}}{\partial x^2}\right) - \frac{1}{2}\left(\frac{\partial W_{\mathrm{I}}}{\partial x}\right)^2\right]\mathrm{d}x\,\mathrm{d}y \tag{24a}$$

$$= -\frac{(3)^{3/4}}{8\pi^2\gamma_0}\varepsilon^{-3/2}\int_0^{2\pi\gamma_0}\int_0^{\pi}\left[\left(\beta^2\frac{\partial^2 F_{\mathrm{II}}}{\partial y^2} - \nu\frac{\partial^2 F_{\mathrm{II}}}{\partial x^2}\right) - \frac{1}{2}\left(\frac{\partial W_{\mathrm{II}}}{\partial x}\right)^2\right]\mathrm{d}x\,\mathrm{d}y \tag{24b}$$

In Eq. (12), we introduce an important parameter ε, which can be re-written as $\varepsilon = \pi^2/(\overline{Z}_B\sqrt{12})$. For a double-walled carbon nanotube we define $\overline{Z}_B = (L^2/R_I t)[1-\nu^2]^{1/2}$, and for a single-walled carbon nanotube we define $\overline{Z}_B = (L^2/Rt)[1-\nu^2]^{1/2}$, that is the Batdorf shell parameter, which should be greater than 2.85 in the case of classical linear buckling analysis (Batdorf, 1947). When $\overline{Z}_B > 2.85$, then $\varepsilon < 1$. It has been shown (Yakobson et al., 1996; Das and Wille, 2002; Liu and Chen, 2003), carbon nanotubes will have large values of $\overline{Z}_B$, so that we always have $\varepsilon \ll 1$. When $\varepsilon < 1$, both Eqs. (13)–(20) are of the boundary layer type and may then be solved by means of a singular perturbation technique. The essence of this procedure, in the present case, is to assume that

$$\begin{aligned} W &= w(x,y,\varepsilon) + \widetilde{W}(x,\xi,y,\varepsilon) + \widehat{W}(x,\zeta,y,\varepsilon) \\ F &= f(x,y,\varepsilon) + \widetilde{F}(x,\xi,y,\varepsilon) + \widehat{F}(x,\zeta,y,\varepsilon) \\ \Psi_x &= \psi_x(x,y,\varepsilon) + \tilde{\Psi}_x(x,\xi,y,\varepsilon) + \hat{\Psi}_x(x,\zeta,y,\varepsilon) \\ \Psi_y &= \psi_y(x,y,\varepsilon) + \tilde{\Psi}_y(x,\xi,y,\varepsilon) + \hat{\Psi}_y(x,\zeta,y,\varepsilon) \end{aligned} \tag{25}$$

where ε is a small perturbation parameter (provided $\overline{Z}_B > 2.85$) as defined in Eq. (12) and $w(x,y,\varepsilon)$, $f(x,y,\varepsilon)$, $\psi_x(x,y,\varepsilon)$, $\psi_y(x,y,\varepsilon)$ are called regular solutions of the shell, $\widetilde{W}(x,\xi,y,\varepsilon)$, $\widetilde{F}(x,\xi,y,\varepsilon)$, $\tilde{\Psi}_x(x,\xi,y,\varepsilon)$, $\tilde{\Psi}_y(x,\xi,y,\varepsilon)$ and $\widehat{W}(x,\zeta,y,\varepsilon)$, $\widehat{F}(x,\zeta,y,\varepsilon)$, $\hat{\Psi}_x(x,\zeta,y,\varepsilon)$, $\hat{\Psi}_y(x,\zeta,y,\varepsilon)$ are the boundary layer solutions near the $x = 0$ and $x = \pi$ edges, respectively, and ξ and ζ are the boundary layer variables, defined as

$$\xi = x/\sqrt{\varepsilon}, \quad \zeta = (\pi - x)/\sqrt{\varepsilon} \tag{26}$$

This means the width of the boundary layers is of order $\sqrt{Rt}$. In Eq. (25) the regular and boundary layer solutions are taken in the forms of perturbation expansions as

$$\begin{aligned} w(x,y,\varepsilon) &= \sum_{j=3} \varepsilon^{j/2} w^{(j/2)}(x,y), \quad f(x,y,\varepsilon) = \sum_{j=0} \varepsilon^j f^{(j)}(x,y) \\ \psi_x(x,y,\varepsilon) &= \sum_{j=1} \varepsilon^j (\psi_x)^{(j)}(x,y), \quad \psi_y(x,y,\varepsilon) = \sum_{j=1} \varepsilon^j (\psi_y)^{(j)}(x,y) \end{aligned} \tag{27a}$$

$$\begin{aligned} \widetilde{W}(x,\xi,y,\varepsilon) &= \sum_{j=1} \varepsilon^{j/2+1} \widetilde{W}^{(j/2+1)}(x,\xi,y), \quad \widetilde{F}(x,\xi,y,\varepsilon) = \sum_{j=1} \varepsilon^{j/2+2} \widetilde{F}^{(j/2+2)}(x,\xi,y) \\ \tilde{\Psi}_x(x,\xi,y,\varepsilon) &= \sum_{j=1} \varepsilon^{(j+3)/2} (\tilde{\Psi}_x)^{(j+3)/2}(x,\xi,y), \quad \tilde{\Psi}_y(x,\xi,y,\varepsilon) = \sum_{j=1} \varepsilon^{j/2+2} (\tilde{\Psi}_y)^{(j/2+2)}(x,\xi,y) \end{aligned} \tag{27b}$$

$$\begin{aligned} \widehat{W}(x,\zeta,y,\varepsilon) &= \sum_{j=1} \varepsilon^{j/2+1} \widehat{W}^{(j/2+1)}(x,\zeta,y), \quad \widehat{F}(x,\zeta,y,\varepsilon) = \sum_{j=1} \varepsilon^{j/2+2} \widehat{F}^{(j/2+2)}(x,\zeta,y) \\ \hat{\Psi}_x(x,\zeta,y,\varepsilon) &= \sum_{j=1} \varepsilon^{(j+3)/2} (\hat{\Psi}_x)^{(j+3)/2}(x,\zeta,y), \quad \hat{\Psi}_y(x,\zeta,y,\varepsilon) = \sum_{j=1} \varepsilon^{j/2+2} (\hat{\Psi}_y)^{(j/2+2)}(x,\zeta,y) \end{aligned} \tag{27c}$$

The initial buckling mode is assumed to have the form

$$w_{\mathrm{I}}^{(2)}(x,y) = A_{11}^{(2)} \sin mx \sin ny \tag{28a}$$

$$w_{\mathrm{II}}^{(2)}(x,y) = a_1 A_{11}^{(2)} \sin mx \sin ny \tag{28b}$$

in which a_1 is a constant and can be determined later.

Substituting Eqs. (25)–(27) into Eqs. (13)–(20), and collecting terms of the same order of ε, we obtain three sets of perturbation equations for the regular and boundary layer solutions, respectively, the details of which may be found in Shen (2002).

Then using Eqs. (28a) and (28b) to solve these perturbation equations of each order, and matching the regular solutions with the boundary layer solutions at each end of the shell, we obtain the asymptotic solutions. For the outer tube, they are

$$W_{\mathrm{I}} = \varepsilon^{3/2}\left[A_{00}^{(3/2)} - A_{00}^{(3/2)}\left(\cos\phi\frac{x}{\sqrt{\varepsilon}} + a_{10}^{(1)}\sin\phi\frac{x}{\sqrt{\varepsilon}}\right)\exp\left(-\alpha\frac{x}{\sqrt{\varepsilon}}\right) - A_{00}^{(3/2)}\left(\cos\phi\frac{\pi-x}{\sqrt{\varepsilon}} + a_{10}^{(1)}\sin\phi\frac{\pi-x}{\sqrt{\varepsilon}}\right)\times\exp\left(-\alpha\frac{\pi-x}{\sqrt{\varepsilon}}\right)\right] + \varepsilon^2[A_{11}^{(2)}\sin mx\sin ny] + \varepsilon^4[A_{00}^{(4)} + A_{20}^{(4)}\cos 2mx + A_{02}^{(4)}\cos 2ny] + \mathrm{O}(\varepsilon^6) \tag{29}$$

$$F_{\mathrm{I}} = -B_{00}^{(0)}\frac{y^2}{2} - \left(C_1 + \beta^2 C_{00}^{(0)}\right)\frac{x^2}{2} + \varepsilon^2\left[-B_{00}^{(2)}\frac{y^2}{2} - \beta^2 C_{00}^{(2)}\frac{x^2}{2} + B_{11}^{(2)}\sin mx\sin ny\right] + \varepsilon^{5/2}\left[A_{00}^{(3/2)}\left(b_{01}^{(5/2)}\cos\phi\frac{x}{\sqrt{\varepsilon}} + b_{10}^{(5/2)}\sin\phi\frac{x}{\sqrt{\varepsilon}}\right)\exp\left(-\alpha\frac{x}{\sqrt{\varepsilon}}\right) + A_{00}^{(3/2)}\left(b_{01}^{(5/2)}\cos\phi\frac{\pi-x}{\sqrt{\varepsilon}} + b_{10}^{(5/2)}\sin\phi\frac{\pi-x}{\sqrt{\varepsilon}}\right)\exp\left(-\alpha\frac{\pi-x}{\sqrt{\varepsilon}}\right)\right] + \varepsilon^4\left[-B_{00}^{(4)}\frac{y^2}{2} - \beta^2 C_{00}^{(4)}\frac{x^2}{2} + B_{20}^{(4)}\cos 2mx + B_{02}^{(4)}\cos 2ny\right] + \mathrm{O}(\varepsilon^6) \tag{30}$$

$$\Psi_{x\mathrm{I}} = \varepsilon^2\left[\left(c_{01}^{(2)}\cos\phi\frac{x}{\sqrt{\varepsilon}} + c_{10}^{(2)}\sin\phi\frac{x}{\sqrt{\varepsilon}}\right)\exp\left(-\alpha\frac{x}{\sqrt{\varepsilon}}\right) + \left(c_{01}^{(2)}\cos\phi\frac{\pi-x}{\sqrt{\varepsilon}} + c_{10}^{(2)}\sin\phi\frac{\pi-x}{\sqrt{\varepsilon}}\right)\times\exp\left(-\alpha\frac{\pi-x}{\sqrt{\varepsilon}}\right)\right] + \varepsilon^3[C_{11}^{(3)}\cos mx\sin ny] + \varepsilon^5[C_{20}^{(5)}\sin 2mx] + \mathrm{O}(\varepsilon^6) \tag{31}$$

$$\Psi_{y\mathrm{I}} = \varepsilon^3[D_{11}^{(3)}\sin mx\cos ny] + \varepsilon^5[D_{02}^{(5)}\sin 2ny] + \mathrm{O}(\varepsilon^6) \tag{32}$$

Note that the effect of boundary layer solutions is negligible in the higher order terms, so that it does not appear in Eq. (32). Then for the inner tube it is just necessary to replace $-C_1$ and $B_{00}^{(j)}$ in Eq. (30) with $+C_1$ and $b_{00}^{(j)}$, and omitting $C_{00}^{(j)}$. Because $B_{00}^{(j)}$ and $b_{00}^{(j)}$ $(j = 0, 2, 4)$ have different values, the axial stress resultants $N_{x\mathrm{I}}$ and $N_{x\mathrm{II}}$ are unequal. Also we need to replace $A_{ik}^{(j)}$, $B_{ik}^{(j)}$, $C_{ik}^{(j)}$ and $D_{ik}^{(j)}$ in Eqs. (29)–(32) with $\bar{A}_{ik}^{(j)}$, $\bar{B}_{ik}^{(j)}$, $\bar{C}_{ik}^{(j)}$ and $\bar{D}_{ik}^{(j)}$, so that the asymptotic solutions W_{II}, F_{II}, $\Psi_{x\mathrm{II}}$ and $\Psi_{y\mathrm{II}}$ have a similar form.

Note that, all of the coefficients in the above equations are related and can be expressed in terms of $A_{11}^{(2)}$, but for the sake of brevity the detailed expressions are not shown, whereas α and ϕ are given in detail in Appendix A.

Because the end-shortening displacements of the outer and inner tubes are identical, upon substitution of F_I and F_{II} into Eqs. (24a) and (24b), we have

$$a_1 = \frac{1}{2B_1}\left\{\left[(B_2)^2 + 4B_1B_3\right]^{1/2} - B_2\right\} \tag{33}$$

All symbols used in Eq. (33) and Eqs. (34)–(36) below are also described in detail in Appendix A. From Eqs. (33) and (A.1) below, it is evident that $a_1 < 1$, then inner tube has a lower amplitude than the outer tube. This follows from the fact that, due to the van der Waals interaction forces, the outer tube is subjected to internal pressure and the inner tube is subjected to external pressure.

Next, upon substitution of F_I and F_{II} into the boundary condition (22d) and F_I and W_I into closed condition (23) and Eq. (24a), the postbuckling equilibrium paths can be written as

$$\lambda_q = \frac{1}{4}(3)^{3/4}\varepsilon^{-3/2}[\lambda_q^{(0)} + \lambda_q^{(2)}(A_{11}^{(2)}\varepsilon^2)^2 + \cdots] \tag{34}$$

and

$$\delta_q = \delta_q^{(0)} + \delta_q^{(2)}(A_{11}^{(2)}\varepsilon^2)^2 + \cdots \tag{35}$$

In Eqs. (34) and (35), $(A_{11}^{(2)}\varepsilon^2)$ is taken as the second perturbation parameter relating to the dimensionless maximum deflection. If the maximum deflection is assumed to be at the point $(x, y) = (\pi/2m, \pi/2n)$, from Eq. (29) we have

$$A_{11}^{(2)}\varepsilon^2 = W_m - \Theta_1 W_m^2 + \cdots \tag{36a}$$

where W_m is the dimensionless form of the maximum deflection of the outer tube that can be expressed as

$$W_m = \left[\varepsilon\frac{\overline{W}}{t}[12(1-\nu^2)]^{1/2} - \Theta_2\right] \tag{36b}$$

Eqs. (34)–(36) are employed to obtain numerical results for full nonlinear postbuckling load-shortening or load-deflection curves of double-walled carbon nanotubes under external hydrostatic pressure, from which results for single-walled carbon nanotubes are obtained as a limiting case. The initial buckling load can readily be obtained numerically, by setting $\overline{W}/t = 0$ (note that $W_m \neq 0$). In this case, the minimum buckling load is determined by considering Eq. (34) for various values of the buckling mode (m, n), which determine the number of half-waves in the X-direction and of full waves in the Y-direction. Note that because of Eq. (29), the prebuckling deformation of the shell is nonlinear.

4. Numerical results and discussion

Numerical results are presented in this section for double-walled carbon nanotubes with different values of shell parameter. As mentioned before, there are no numerical and experimental results available in the literature, including previous works of Ru (Wang et al., 2003a) and Yakobson (Yakobson et al., 1996), for the buckling of the single-walled and/or double-walled carbon nanotubes under hydrostatic pressure, no direct comparison is made in this section.

Before we go to the discussion of the postbuckling response of double-walled carbon nanotubes under hydrostatic pressure, let us first examine the buckling pressure of the double-walled carbon nanotube. From Eq. (A.2c), and neglecting prebuckling deformations, one has

$$q = \frac{q_{cl}}{(n^2\beta^2 + 0.5m^2)}\left\{\left[\frac{m^4}{g_{06}}\frac{1+\gamma_0}{\gamma_0} - C_1 n^2\beta^2(1-\gamma_0)\right] + \left[g_{08}(1+\gamma_0) - \frac{C_0(1-a_1)^2}{a_1}\right]\frac{\pi^4}{12\overline{Z}_B^2}\right\} \tag{37}$$

where the critical pressure can be computed exactly with buckling mode (m, n). In particular, for single-walled carbon nanotube without van der Waals forces, the critical pressure can be given by

$$q = \frac{q_{cl}}{(n^2\beta^2 + 0.5m^2)}\left[\frac{m^4}{g_{06}} + g_{08}\frac{\pi^4}{12\overline{Z}_B^2}\right] \tag{38}$$

From Eqs. (37) and (38), it can be seen that the critical pressure for the double-walled carbon nanotube is higher than that associated with the single-walled carbon nanotube with the same outside diameter and material properties. In fact, for multi-walled carbon nanotubes the outside diameter increases as the number of layers increases (Lu, 1997), and the material properties are dependent on the layer number (Tu and Ou-Yang, 2002).

Note that for thin shell model we have $g_{08} = g_{06} = (m^2 + n^2\beta^2)^2$, then relation (38) reduces to the classical result (Timoshenko and Gere, 1961)

$$q = \frac{q_{cl}}{(n^2\beta^2 + 0.5m^2)}\left[\frac{m^4}{(m^2 + n^2\beta^2)^2} + (m^2 + n^2\beta^2)^2\frac{\pi^4}{12\overline{Z}_B^2}\right] \tag{39}$$

Taking this fact into account, we expect that Eq. (38) agrees well with molecular-dynamics simulations for single-walled nanotubes.

Based on the continuum assumption, the key problem in computing is to determine the wall thickness of the nanotube. Recently, Tu and Ou-Yang (2002) found that the effective Young's modulus of the multi-walled carbon nanotube is an apparent function of the number of layers, N, varying from 4.70 to 1.04 TPa for $N = 1$ to ∞. They provided that the wall thickness of a single-walled carbon nanotube is 0.075 nm, Poisson's ratio $v = 0.34$ and Young's modulus $E = 4.70$ TPa, whereas for a double-walled carbon nanotube $E = 1.70$ TPa. This value is close to that of experimental results of Treacy et al. (1996), and is used in the following computation. For the sake of illustration, we consider the initial interlayer spacing between the inner and outer tube is 0.34 nm, as mentioned before, in such a case the initial pressure p_0 is zero or $C_1 = 0$. The van der Waals interaction constant is taken as $C = 99.187$ GPa/nm (Wang et al., 2003a,b).

The buckling pressure q_{cr} (in GPa) for simply supported, double-walled carbon nanotubes subjected to hydrostatic pressure are calculated and compared in Table 1. Three test examples are considered. Examples 1 and 2 are moderately thick double-walled carbon nanotubes, they have $R_I = 1.095$ nm, $R_{II} = 0.68$ nm and $R_I = 1.415$ nm, $R_{II} = 1.0$ nm, respectively, while Example 3 is a thin double-walled carbon nanotube, which has $R_I = 3.415$ nm and $R_{II} = 3.0$ nm. In Table 1 the single-walled carbon nanotube with $R = R_I$ for each case is treated as a comparator. In computation, the shell length-to-radius ratio $L/R_{II} = 10$ and each shell thickness is taken as $t = 0.075$ nm. The results show that the buckling pressure for the single-walled carbon nanotube is higher than that of the double-walled carbon nanotube, due to the high value of Young's modulus $E = 4.70$ TPa. The results also confirm that the critical pressure for the double-walled carbon nanotube is higher than that of the single-walled carbon nanotube under the same conditions.

We now turn our attention to the postbuckling behavior of a double-walled carbon nanotube subjected to hydrostatic pressure. Fig. 2 compares the postbuckling behavior for the same three double-walled carbon nanotubes as shown in Table 1. It is seen that the load-shortening curves seem linear, whereas the load-deflection curves are really nonlinear. The results show that the postbuckling equilibrium path becomes lower when the nanotube becomes thinner.

Table 1
Comparisons of buckling pressure for carbon nanotubes ($v = 0.34$, $L/R_{II} = 10$, $t = 0.075$ nm)

Example	E (TPa)		Mean radius (nm)	q_{cr} (GPa)
1	1.7	Double-walled	$R_I = 1.095$, $R_{II} = 0.68$	0.6267 (1,2)[a]
	1.7	Single-walled	$R = 1.095$	0.3265 (1,2)
	4.7	Single-walled	$R = 1.095$	0.9026 (1,2)
2	1.7	Double-walled	$R_I = 1.415$, $R_{II} = 1.0$	0.2915 (1,2)
	1.7	Single-walled	$R = 1.415$	0.1509 (1,2)
	4.7	Single-walled	$R = 1.415$	0.4172 (1,2)
3	1.7	Double-walled	$R_I = 3.415$, $R_{II} = 3.0$	0.0322 (1,2)
	1.7	Single-walled	$R = 3.415$	0.0159 (1,2)
	4.7	Single-walled	$R = 3.415$	0.0440 (1,2)

[a] The numbers in brackets indicate the buckling mode (m, n).

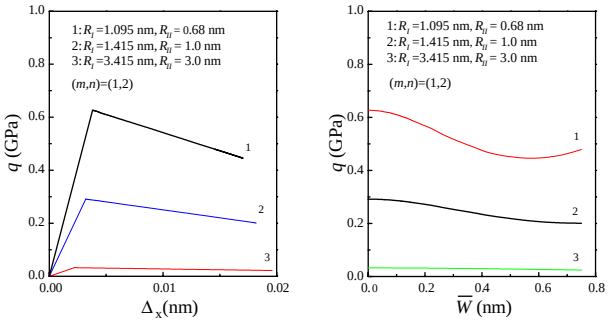

Fig. 2. Postbuckling behavior for double-walled carbon nanotubes under hydrostatic pressure ($E = 1.7$ TPa, $v = 0.34$, $L/R_{II} = 10$, $t = 0.075$ nm; 1: $R_I = 1.095$ nm, $R_{II} = 0.68$ nm; 2: $R_I = 1.415$ nm, $R_{II} = 1.0$ nm; 3: $R_I = 3.415$ nm, $R_{II} = 3.0$ nm).

Fig. 3 compares the postbuckling behaviors for single-walled and double-walled carbon nanotubes of Example 1. It can be seen that, for the single-walled carbon nanotube, an increase in pressure is usually required to obtain an increase in deformation, and the postbuckling equilibrium path is stable. In contrast, for the double-walled carbon nanotube the load decreases as end-shortening increases, and the postbuckling path is unstable. Note that in the present example $E = 1.70$ TPa is for the double-walled carbon nanotube, whereas $E = 4.70$ TPa is for the single-walled carbon nanotube.

A large variation of Young's moduli was reported in the open literature (Treacy et al., 1996; Wong et al., 1997; Lourie and Wagner, 1998; Muster et al., 1998; Yu et al., 2000). We are not aware of the exact value of the Young's modulus E for a single-walled carbon nanotube. Fig. 4 shows the postbuckling equilibrium paths for single-walled and double-walled carbon nanotubes with the fixed Young's modulus $E = 1.0$ TPa and $v = 0.27$. The shell geometric parameters are taken as in Example 1. In such a case, for the double-walled carbon nanotube the buckling pressure $q_{cr} = 0.36$ GPa, while for the single-walled carbon nanotube the buckling pressure $q_{cr} = 0.19$ GPa. The results confirm that both buckling pressure and postbuckling load-deflection curve for the double-walled carbon nanotube are higher than those of the single-walled

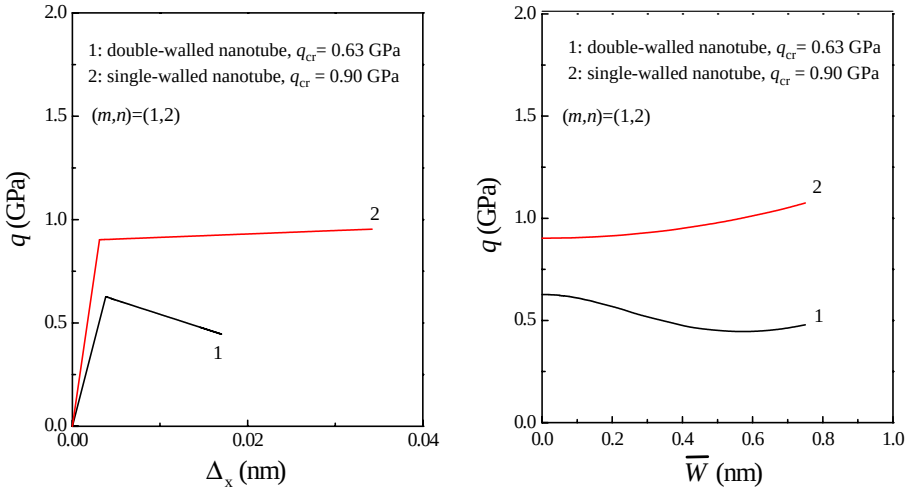

Fig. 3. Postbuckling behavior for carbon nanotubes under hydrostatic pressure ($L = 6.8$ nm, $t = 0.075$ nm; 1: $R_I = 1.095$ nm, $R_{II} = 0.68$ nm, $E = 1.7$ TPa, $v = 0.34$, 2: $R = 1.095$ nm, $E = 4.7$ TPa, $v = 0.34$).

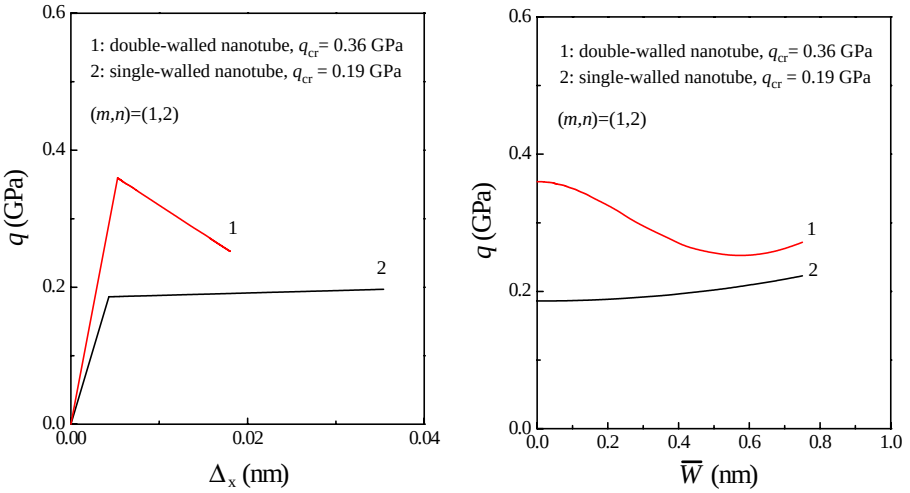

Fig. 4. Postbuckling behavior for carbon nanotubes under hydrostatic pressure ($E = 1.0$ TPa, $v = 0.27$, $L = 6.8$ nm, $t = 0.075$ nm; 1: $R_I = 1.095$ nm, $R_{II} = 0.68$ nm; 2: $R = 1.095$ nm).

carbon nanotube under the same conditions. Accordingly, if the experimental results show that the buckling load of a double-walled carbon nanotube is higher than that of the single-walled carbon nanotube, we believe that the Young's moduli of these tubes are to have the same value. In contrast, if the experimental results show that the buckling load of a single-walled carbon nanotube is higher than that of the double-walled carbon nanotube, then we believe that the Young's modulus of the single-walled carbon nanotube should be higher than that of the double-walled carbon nanotube.

5. Conclusions

At the conclusion of this work, we now know two different special postbuckling behaviors of carbon nanotubes under hydrostatic pressure. The single-walled carbon nanotube will have a stable postbuckling path, whereas the double-walled carbon nanotube will have an unstable postbuckling behavior due to the presence of van der Waals interaction forces.

It has been reported (Zhou, 1994) that multi-walled carbon nanotubes contain significant concentrations of defects. According to Figs. 2–4, we come to believe that the pressure-loaded double-walled carbon nanotube is imperfection-sensitive, and the simulation of a local defect needs to be developed.

The results presented provide a framework for the postbuckling prediction of double-walled carbon nanotubes subjected to external hydrostatic pressure based on a continuum mechanics model. Verification of this theoretical prediction poses an interesting research topic for further work.

Acknowledgements

This work is supported in part by the National Natural Science Foundation of China under Grant 50375091. The author is grateful for this financial support.

Appendix A

In Eq. (33)

$$B_1 = \frac{1}{1+\gamma_0}\frac{m^2(0.5-v)}{n^2\beta^2+0.5m^2}$$

$$B_2 = \frac{1}{\gamma_0} - \frac{2}{1+\gamma_0}\frac{m^2(0.5-v)}{n^2\beta^2+0.5m^2} + \frac{m^2}{C_0}\left\{\left[\frac{m^2}{\gamma_0 g_{06}}\left(\frac{1}{\gamma_0} - \frac{m^2(0.5-v)}{n^2\beta^2+0.5m^2}\right) + C_1\frac{n^2\beta^2}{m^2}\left(1+\frac{1-\gamma_0}{1+\gamma_0}\frac{m^2(0.5-v)}{n^2\beta^2+0.5m^2}\right)\right.\right.$$
$$\left.\left. + \frac{2vC_1}{1+\gamma_0}\right]\varepsilon^{-2} + \frac{g_{08}}{m^2}\left(1 - \frac{m^2(0.5-v)}{n^2\beta^2+0.5m^2}\right)\right\}$$

$$B_3 = \frac{1}{\gamma_0} - \frac{1}{1+\gamma_0}\frac{m^2(0.5-v)}{n^2\beta^2+0.5m^2} \tag{A.1}$$

and in Eqs. (34)–(36)

$$\Theta_1 = \left[\frac{1}{8}n^2\beta^2 + \frac{1}{8}n^2\beta^2\frac{g_{06}+8m^4}{\Delta_2} - \frac{1}{4}\frac{m^4(n^2\beta^2+0.5m^2)}{\Delta_1} + \left(1 - v\frac{0.5+v\gamma_0}{1+\gamma_0}\right)\lambda_q^{(2)}\right] \tag{A.2a}$$

$$\Theta_2 = \left(1 - v\frac{0.5+v\gamma_0}{1+\gamma_0}\right)\lambda_q^{(0)} + C_1\left(1 - v\frac{2\gamma_0}{1+\gamma_0}\right) \tag{A.2b}$$

$$\lambda_q^{(0)} = \frac{1}{(n^2\beta^2+0.5m^2)}\left\{\left[\frac{m^4}{g_{06}}\frac{1+\gamma_0}{\gamma_0} - C_1n^2\beta^2(1-\gamma_0)\right] + \left[g_{08}(1+\gamma_0) - \frac{C_0(1-a_1)^2}{a_1}\right]\varepsilon^2\right\} \tag{A.2c}$$

$$\lambda_q^{(2)} = \frac{1}{(n^2\beta^2+0.5m^2)}\left\{\frac{1}{16}m^4(1+a_1^2\gamma_0) + \frac{m^4n^2\beta^2}{g_{06}}\frac{m^4(n^2\beta^2+0.5m^2)}{\Delta_1}g_{21} - \frac{m^4n^4\beta^4}{2g_{06}}\left[\frac{g_{06}+8m^4}{\Delta_2}\right.\right.$$
$$\left.\left. + a_1^2\gamma_0\frac{g_{06}+8m^8}{(1-4n^2\beta^2C_1\gamma_0^2)g_{06}-4m^4}\right] - \frac{1}{4}n^4\beta^4\left[\frac{\Delta_3}{\Delta_2} + a_1^2\gamma_0\frac{3m^4+n^2\beta^2C_1\gamma_0^2g_{06}}{(1-4n^2\beta^2C_1\gamma_0^2)g_{06}-4m^4}\right]\right\} \tag{A.2d}$$

$$\delta_q^{(0)} = \left[\frac{0.5-v}{1+\gamma_0} + \frac{v}{\alpha\pi}\left(1 - v\frac{0.5+v\gamma_0}{1+\gamma_0}\right)\varepsilon^{1/2}\right]\lambda_q - \frac{(3)^{3/4}}{4}C_1v\left[\frac{1-\gamma_0}{1+\gamma_0} - \frac{1}{\alpha\pi}\left(1 - v\frac{2\gamma_0}{1+\gamma_0}\right)\varepsilon^{1/2}\right]\varepsilon^{-3/2}$$
$$+ \frac{(3)^{3/4}}{16}\frac{\alpha}{\pi}\left[C_1\left(1 - v\frac{2\gamma_0}{1+\gamma_0}\right)\varepsilon^{-3/2} + \left(1 - v\frac{0.5+v\gamma_0}{1+\gamma_0}\right)\frac{4}{(3)^{3/4}}\lambda_q\right]^2\varepsilon \tag{A.2e}$$

$$\delta_q^{(2)} = \frac{(3)^{3/4}}{32}m^2\varepsilon^{-3/2} \tag{A.2f}$$

in the above equations

$$
\begin{aligned}
\Delta_1 &= \left(\frac{1+\gamma_0}{\gamma_0}\right)m^4 + C_1 g_{06}(\gamma_0 n^2\beta^2 + 0.5m^2)\\
\Delta_2 &= \left[1 - 4m^2 C_1\left(\frac{2\nu\gamma_0}{1+\gamma_0} - \frac{1-\gamma_0}{1+\gamma_0}\frac{n^2\beta^2(0.5+\nu\gamma_0)}{n^2\beta^2+0.5m^2}\right)\right]g_{06} - 4m^4\left(\frac{0.5+\nu\gamma_0}{1+\gamma_0}\frac{m^2}{n^2\beta^2+0.5m^2}\right)\\
\Delta_3 &= \left(2 + \frac{0.5+\nu\gamma_0}{\gamma_0}\frac{m^2}{n^2\beta^2+0.5m^2}\right)m^4 + m^2 C_1 g_{06}\left(\frac{2\nu\gamma_0}{1+\gamma_0} - \frac{1-\gamma_0}{1+\gamma_0}\frac{n^2\beta^2(0.5+\nu\gamma_0)}{n^2\beta^2+0.5m^2}\right)\\
g_{06} &= (m^2+n^2\beta^2)^2\\
g_{08} &= (\gamma_{110}m^4 + 2\gamma_{112}m^2n^2\beta^2 + \gamma_{114}n^4\beta^4)\\
&\quad + \frac{m^2(\gamma_{120}m^2 + \gamma_{122}n^2\beta^2)g_{04} + n^2\beta^2(\gamma_{131}m^2 + \gamma_{133}n^2\beta^2)g_{03}}{g_{00}}\\
g_{00} &= (\gamma_{31} + \gamma_{320}m^2 + \gamma_{322}n^2\beta^2)(\gamma_{41} + \gamma_{430}m^2 + \gamma_{432}n^2\beta^2) - \gamma_{331}^2 m^2 n^2\beta^2\\
g_{03} &= (\gamma_{31} + \gamma_{320}m^2 + \gamma_{322}n^2\beta^2)(\gamma_{41} - \gamma_{411}m^2 - \gamma_{413}n^2\beta^2)\\
&\quad - \gamma_{331}m^2(\gamma_{31} - \gamma_{310}m^2 - \gamma_{312}n^2\beta^2)\\
g_{04} &= (\gamma_{41} + \gamma_{430}m^2 + \gamma_{432}n^2\beta^2)(\gamma_{31} - \gamma_{310}m^2 - \gamma_{312}n^2\beta^2)\\
&\quad - \gamma_{331}n^2\beta^2(\gamma_{41} - \gamma_{411}m^2 - \gamma_{413}n^2\beta^2)\\
g_{41} &= \frac{\gamma_{41} - \gamma_{413}4n^2\beta^2}{\gamma_{41} + \gamma_{432}4n^2\beta^2}, \quad g_{21} = \frac{\gamma_0(\gamma_{114} + \gamma_{133}g_{41})16n^4\beta^4 + 2C_0}{\gamma_0(\gamma_{114} + \gamma_{133}g_{41})16n^4\beta^4 + C_0}\\
\alpha &= \phi = \left[\frac{b}{2}\right]^{1/2}, \quad b = \left[\frac{\gamma_{320}^2}{\gamma_{320}\gamma_{110} - \gamma_{310}\gamma_{120}}\right]^{1/2}
\end{aligned}
\tag{A.3}
$$

References

Batdorf, S.B., 1947. A simplified method of elastic-stability analysis for thin cylindrical shells. NACA TR-874.

Cumings, J., Zettl, A., 2000. Low-friction nanoscale linear bearing realized from multiwall carbon nanotubes. Science 289, 602–604.

Das, P.S., Wille, L.T., 2002. Atomistic and continuum studies of carbon nanotubes under pressure. Computational Materials Science 24, 159–162.

Girifalco, L.A., 1991. Interaction potential for C_{60} molecules. Journal of Physical Chemistry 95, 5370–5371.

Girifalco, L.A., Lad, R.A., 1956. Energy of cohesion, compressibility, and the potential energy functions of graphite system. Journal of Chemical Physics 25, 693–697.

Harik, V.M., 2002. Mechanics of nanotubes: applicability of the continuum-beam models. Computational Materials Science 24, 328–342.

Hertel, T., Walkup, R.E., Avouris, P., 1998. Deformation of carbon nanotubes by surface van der Waals forces. Physical Review B 58, 13870–13873.

Iijima, S., 1991. Helical microtubes of graphitic carbon. Nature 354, 56–58.

Kolmogorov, A.N., Crespi, V.H., 2000. Smoothest bearings: interlayer sliding in multiwalled carbon nanotubes. Physical Review Letters 85, 4727–4730.

Liu, B.B., Sundqvist, B., Andersson, O., Wågberg, T., Nyeanchi, E.B., Zhu, X.-M., Zou, G., 2001. Electric resistance of single-walled carbon nanotubes under hydrostatic pressure. Solid State Communications 118, 31–36.

Liu, Y.J., Chen, X.L., 2003. Evaluations of the effective material properties of carbon nanotube-based composites using a nanoscale representative volume element. Mechanics of Materials 35, 69–81.

Lourie, O., Wagner, H.D., 1998. Evaluation of Young's modulus of carbon nanotubes by micro-Raman spectroscopy. Journal of Materials Research 13, 2418–2422.

Lu, J.P., 1997. Elastic properties of single and multilayered nanotubes. Journal of Physics and Chemistry of Solids 58, 1649–1652.

Muster, J., Burghard, M., Roth, S., Duesberg, G.S., Hernández, E., Rubio, A., 1998. Scanning force microscopy characterization of individual carbon nanotubes on electrode arrays. Journal of Vacuum Science and Technology B 16, 2796–2801.

Qian, D., Wagner, G.J., Liu, W.K., Yu, M.-F., Ruoff, R.S., 2002. Mechanics of carbon nanotubes. Applied Mechanics Review 66, 495–533.

Reddy, J.N., Liu, C.F., 1985. A higher-order shear deformation theory of laminated elastic shells. International Journal of Engineering Science 23, 319–330.

Reich, S., Jantoljak, H., Thomsen, C., 2000. Shear strain in carbon nanotubes under hydrostatic pressure. Physical Review B 61, 13389–13392.

Reich, S., Thomsen, C., Ordejón, P., 2002. Elastic properties of carbon nanotubes under hydrostatic pressure. Physical Review B 65, 153404.

Ru, C.Q., 2000a. Elastic buckling of single-walled carbon nanotube ropes under high pressure. Physical Review B 62, 10405–10408.

Ru, C.Q., 2000b. Effect of van der Waals forces on axial buckling of a double-walled carbon nanotube. Journal of Applied Physics 87, 7227–7231.

Ru, C.Q., 2001. Axially compressed buckling of a doublewalled carbon nanotube embedded in an elastic medium. Journal of the Mechanics and Physics of Solids 49, 1265–1279.

Ruoff, R.S., Tersoff, J., Lorents, D.C., Subramoney, S., Chan, B., 1993. Radial deformation of carbon nanotubes by van der Waals forces. Nature 364, 514–516.

Shen, H.-S., 2001. Postbuckling of shear deformable cross-ply laminated cylindrical shells under combined external pressure and axial compression. International Journal of Mechanical Sciences 43, 2493–2523.

Shen, H.-S., 2002. Postbuckling Behavior of Plates and Shells (in Chinese). Science and Technological Press, Shanghai, China.

Shen, H.-S., Chen, T.-Y., 1988. A boundary layer theory for the buckling of thin cylindrical shells under external pressure. Applied Mathematics and Mechanics 9, 557–571.

Shen, H.-S., Chen, T.-Y., 1990. A boundary layer theory for the buckling of thin cylindrical shells under axial compression. In: Chien, W.Z., Fu, Z.Z. (Eds.), Advances in Applied Mathematics and Mechanics in China, Vol. 2. International Academic Publishers, Beijing, China, pp. 155–172.

Tang, J., Qin, L.-C., Sasaki, T., Yudasaka, M., Matsushita, A., Iijima, S., 2000. Compressibility and polygonization of single-walled carbon nanotubes under hydrostatic pressure. Physical Review Letters 85, 1887–1889.

Tang, J., Qin, L.-C., Sasaki, T., Yudasaka, M., Matsushita, A., Iijima, S., 2002. Revealing properties of single-walled carbon nanotubes under high pressure. Journal of Physics: Condensed Matter 14, 10575–10578.

Timoshenko, S.P., Gere, J.M., 1961. Theory of Elastic Stability. McGraw-Hill, New York.

Thostenson, E.K., Ren, Z., Chou, T.-W., 2001. Advances in the science and technology of carbon nanotubes and their composites: a review. Composites Science and Technology 61, 1899–1912.

Treacy, M.M.J., Ebbesen, T.W., Gibson, J.M., 1996. Exceptionally high Young's modulus observed for individual carbon nanotubes. Nature 381, 678–680.

Tu, Z.-C., Ou-Yang, Z.-C., 2002. Single-walled and multiwalled carbon nanotubes viewed as elastic tubes with the effective Young's moduli dependent on layer number. Physical Review B 65, 233407.

Wang, C.Y., Ru, C.Q., Mioduchowski, A., 2003a. Elastic buckling of multiwall carbon nanotubes under high pressure. Journal of Nanoscience and Nonatechnology 3, 199–208.

Wang, C.Y., Ru, C.Q., Mioduchowski, A., 2003b. Axially compressed buckling of pressured multiwall carbon nanotubes. International Journal of Solids and Structures 40, 3893–3911.

Wong, E.W., Sheehan, P.E., Lieber, C.M., 1997. Nanobeam mechanics: elasticity, strength, and toughness of nanorods and nanotubes. Science 277, 1971–1975.

Yakobson, B.I., Brabec, C.J., Bernholc, J., 1996. Nanomechanics of carbon tubes: instability beyond linear response. Physical Review Letters 76, 2511–2514.

Yu, M.F., Lourie, O., Dyer, M.J., Moloni, K., Kelly, T.F., Ruoff, R.S., 2000. Strength and breaking mechanism of multiwalled carbon nanotubes under tensile load. Science 287, 637–640.

Zhou, O., 1994. Defects in carbon nanostructures. Science 263, 1744–1747.